

Synthesis and structures of two new Cu(I) frameworks bearing 1,3-bis(4-pyridyl)propane and inorganic linkers

ZHAOBO HU^a, BO LI^{b,*}, WENQIANG JU^a, YUNING LIANG^a and ZILU CHEN^{a,*}

^aState Key Laboratory for the Chemistry and Molecular Engineering of Medicinal Resources, School of Chemistry and Pharmaceutical Sciences, Guangxi Normal University, Guilin 541004, P R China

^bCollege of Chemistry and Pharmaceutical Engineering, Nanyang Normal University, Nanyang 473061, P R China
e-mail: zlchen@mailbox.gxnu.edu.cn; libozzu0107@163.com

MS received 21 January 2016; revised 21 April 2016; accepted 24 April 2016

Abstract. Two novel metal-organic coordination polymers [Cu₂(bpp)Cl₂] (**1**) and [Cu₂(bpp)₂SO₄]·DMF·3H₂O (**2**) were prepared from the reactions of 1,3-bis(4-pyridyl)propane (bpp) with CuCl₂ and CuSO₄, respectively, which were characterized by single-crystal X-ray diffraction analysis, elemental analysis, IR spectroscopy and powder X-ray diffraction analysis. **1** features inorganic one-dimensional [Cu₂Cl₂] ribbons, which are linked by the bpp ligands to form a three-dimensional metal-organic framework exhibiting a 3,3,4-connected 3-nodal topology. **2** presents [Cu₂SO₄] inorganic dinuclear secondary building blocks which are further connected by the bpp ligands to construct a two-dimensional framework featuring flask-stacking appearance. They are typical examples of metal-organic framework constructed by the synergistic use of organic and inorganic linkers.

Keywords. Crystal structure; 1,3-bis(4-pyridyl)propane; Cu(I); inorganic linker; organic linker.

1. Introduction

Coordination polymers, which present one- to three-dimensional topologies, underwent a rapid development in the past decades for their aesthetic structures and interesting properties such as magnetism, catalysis, and non-linear optics.^{1–7} Now the targeted coordination polymers can be constructed under control on demand by designing appropriate linkers and metal nodes or cluster-based nodes. Among them, the construction of metal-organic frameworks (MOFs) attracts special interest because of their porous structure and potential applications in various areas such as gas storage, separation, and catalysis.^{8–10} Thus, a lot of MOFs spring up like mushrooms, some of which exhibit certain conformational effects such as breathing effects.^{11–18} As is well known, one of the key factors for the construction of MOFs is the design and selection of appropriate linkers which link the metal ions or secondary building units into the targeted MOFs. Most of the recent studies concentrate on the organic linkers with a certain skeleton and various functional groups.^{19–24} However, the uses of inorganic linkers or a combination of organic and inorganic linkers to construct MOFs are

rarely reported. The synergistic effect of inorganic and organic linkers in one MOF material might bring about new types of topologies, as well as endow the targeted materials with new functions. To achieve this goal, it is necessary to carry out a systematic investigation on this kind of MOF materials.

Based on the above-mentioned background, we chose 1,3-bis(4-pyridyl)propane (bpp) as the organic linker and chloride or sulfate ions as the inorganic linker to make this study. Herein, we present the structures of one three-dimensional framework [Cu₂(bpp)Cl₂] (**1**) and one flask-stacking two-dimensional framework [Cu₂(bpp)₂SO₄]·DMF·3H₂O (**2**).

2. Experimental Section

2.1 Materials and instrumentation

All reagents were used as obtained without further purification. The infrared spectra were recorded from KBr pellets in the range 4000–400 cm^{–1} with a Perkin-Elmer Spectrum One FT-IR spectrometer. Elemental analyses (C, H, N) were performed with a Perkin-Elmer 2400II CHN elemental analyzer.

*For correspondence

2.2 Synthesis of the complexes

2.2a Synthesis of $[Cu_2(bpp)Cl_2]$ (1**):** To a 20 cm long Pyrex tube containing 1,3-bis(4-pyridyl)propane (0.08 mmol, 0.0159 g) and $CuCl_2 \cdot 2H_2O$ (0.1 mmol, 0.0170 g) was added methanol (1 mL). After being frozen by liquid nitrogen and subsequent evacuation, it was sealed, warmed and heated at 100°C. 5 d later, it was cooled slowly to ambient temperature over 1 d, yielding yellow crystals of **1** in a yield of 19%. Anal. Calcd. (%) for $C_{13}H_{14}Cl_2Cu_2N_2$: C, 39.41; H, 3.56; N, 7.07. Found (%): C, 39.21; H, 3.26; N, 7.27. IR (KBr, cm^{-1}): 3432m, 3056w, 2930w, 2858w, 2365w, 2336w, 1937w, 1611s, 1553w, 1500w, 1424m, 1382w, 1215w, 1070w, 1024w, 806m, 734w, 616w, 517w.

2.2b Synthesis of $[Cu_2(bpp)_2SO_4] \cdot DMF \cdot 3H_2O$ (2**):** To a 20 cm long Pyrex tube containing 1,3-bis(4-pyridyl)propane (0.08 mmol, 0.0159 g) and $CuSO_4 \cdot 5H_2O$ (0.1 mmol, 0.0250 g) was added DMF (1 mL). After being frozen by liquid nitrogen and subsequent

evacuation, it was sealed, warmed and heated at 100°C. 5 d later, it was cooled slowly to ambient temperature over 1 d, yielding yellow brown crystals of **2** in a yield of 17%. Anal. Calcd. (%) for $C_{29}H_{41}Cu_2N_5O_8S$: C, 46.64; H, 5.53; N, 9.38; S, 4.29. Found (%): C, 46.46; H, 5.20; N, 9.53; S, 3.98. IR (KBr, cm^{-1}): 3444s, 2928w, 2860w, 1661s, 1617s, 1560w, 1501w, 1429m, 1384m, 1284w, 1250w, 1226w, 1221w, 1111s, 858m, 810w, 752w, 603m, 519m.

2.3 X-ray crystallography

The single-crystal X-ray data of **1** and **2** were collected on a Bruker APEX-II CCD diffractometer using the graphite monochromated Mo K_α radiation ($\lambda = 0.71073 \text{ \AA}$) at 298(2) K. Data processing was accomplished with the SAINT processing program. The structure was solved by direct methods and refined on F^2 by full-matrix least squares using SHELXTL.²⁵ All non-hydrogen atoms were refined anisotropically. The crystallographic data and structure refinement details are summarized in table 1.

Table 1. Crystallographic data and structural refinement parameters for **1** and **2**.

	1	2
Formula	$C_{13}H_{14}Cl_2Cu_2N_2$	$C_{29}H_{41}Cu_2N_5O_8S$
fw	396.24	746.81
T / K	153(2)	298(2)
$\lambda / \text{\AA}$	0.71073	0.71073
Crystal system	Orthorhombic	Monoclinic
Space group	$P2_12_12_1$	$C2/c$
$a / \text{\AA}$	6.3873(4)	16.934(2)
$b / \text{\AA}$	9.0571(6)	24.172(3)
$c / \text{\AA}$	24.3181(16)	8.8786(11)
$\alpha / ^\circ$	90	90
$\beta / ^\circ$	90	111.410(4)
$\gamma / ^\circ$	90	90
$V / \text{\AA}^3$	1406.81(16)	3383.5(7)
Z	4	4
$D_c / g \text{ cm}^{-3}$	1.871	1.537
μ / mm^{-1}	3.387	1.372
$F(000)$	792	1552
$\theta / ^\circ$	1.67 to 30.00	2.48 to 25.01
Reflns collected	20418	16861
Reflns unique	4070	2945
R_{int}	0.0215	0.0271
GOF on F^2	1.108	1.118
$R_1 [I > 2\sigma(I)]^{[a]}$	0.0167	0.07709
$wR_2 [I > 2\sigma(I)]^{[b]}$	0.0466	0.1929
R_1 (all data) ^[a]	0.0173	0.0807
wR_2 (all data) ^[b]	0.0468	0.2042
Flack	0.021(7)	
Largest diff. Peak, hole / ($e \text{ \AA}^{-3}$)	0.565 and -0.449	1.642 and -0.907

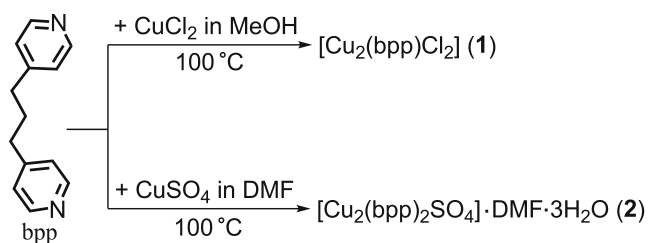
^[a] $R_1 = \Sigma ||F_o| - |F_c|| / \Sigma |F_o|$; ^[b] $wR_2 = [\Sigma w(F_o^2 - F_c^2)^2 / \Sigma w(F_o^2)^2]^{1/2}$.

3. Results and Discussion

3.1 Synthesis and characterization

Complex **1** was obtained from the reaction of 1,3-bis(4-pyridyl)propane (bpp) with CuCl_2 in a molar ratio of 4:5 in CH_3OH at 100°C (scheme 1). Complex **2** was obtained from the reaction of bpp with CuSO_4 in a molar ratio of 4:5 in DMF at 100°C (scheme 1). The Cu(II) ions in the two reactions underwent a reduction into Cu(I) . The mechanism for this transformation is not clear at present. However, the solvents of MeOH and DMF used for the preparation of **1** and **2** might play the role of reducing agents, which were supported by the related cases reported in documents.^{26–30} In order to get pure samples in a reasonable yield, their synthetic conditions were optimized by varying anions, reaction temperatures, solvents and the ratio of $\text{M}^{2+}:\text{bpp}$.

The infrared (IR) spectra (figures S1 and S2, in Supplementary Information) of **1** and **2** were recorded from KBr pellets in the range of $400\text{--}4000\text{ cm}^{-1}$. The bands at 1599 and 1583 cm^{-1} in the spectra are assigned to the $\nu(\text{C}=\text{N})$ in **1** and **2**, respectively.^{18,31} The thermogravimetric analyses were performed in N_2 atmosphere



Scheme 1. A schematic show of the syntheses of **1** and **2**.

at a heating rate of $10^\circ\text{C} \cdot \text{min}^{-1}$ from 30 to 1000°C . It revealed a weight loss of 50.46% between 237 and 568°C as shown in figure S3, which corresponds to the decomposition of the framework of **1**. The TG results (figure S4) show that compound **2** has a weight loss of 17.16% in the temperature range of 35 to 249°C , which corresponds to the loss of three free H_2O and one lattice DMF molecules (calcd 17.02%). Then a weight loss of 53.10% is followed in the temperature range of $250\text{--}496^\circ\text{C}$, which is due to the collapse of the framework of **2**. The recorded experimental PXRD patterns of the two titled compounds agree well with their simulated ones from the single-crystal X-ray diffractive data (figures S5 and S6, in Supplementary Information), which confirms the phase purities of the microcrystals of compounds **1** and **2**.

3.2 Crystal Structures

The crystal structures of **1** and **2** were determined by single-crystal X-ray diffraction analysis. **1** crystallizes in the monoclinic space group $P2_12_12_1$. **2** crystallizes in the monoclinic space group $C2/c$. The related bond lengths and angles of **1** and **2** are listed in tables 2 and 3, respectively.

As shown in figure 1a, the asymmetric unit of **1** is composed of one bpp ligand, two copper atoms and two chloride ions. The two copper centers display different coordination geometries (figure 1a). Cu1 is three-coordinated in an early planar triangular coordination geometry by one N atom from the bpp ligand and two chloride ions. The $\text{Cu1}\text{--N}$ bond length is $1.9897(14)\text{ \AA}$, and the $\text{Cu1}\text{--Cl}$ bond lengths are $2.2229(4)$ and

Table 2. Selected bond lengths / \AA and bond angles / $^\circ$ for **1**.

Cu1--N1	$1.9897(14)$	N1--Cu1--Cl2A	$125.31(4)$
Cu1--Cl2A	$2.2229(4)$	N1--Cu1--Cl1	$111.75(4)$
Cu1--Cl1	$2.3116(4)$	Cl2A--Cu1--Cl1	$120.119(17)$
Cu1--Cu2	$2.9685(3)$	N2B--Cu2--Cl1	$125.57(4)$
Cu2--N2B	$2.0022(13)$	N2B--Cu2--Cl2	$112.63(4)$
Cu2--Cl1	$2.3465(4)$	Cl1--Cu2--Cl2	$104.644(15)$
Cu2--Cl2	$2.3624(5)$	N2B--Cu2--Cl1A	$99.59(4)$
Cu2--Cl1A	$2.5107(4)$	Cl1--Cu2--Cl1A	$101.023(12)$
Cl1--Cu2C	$2.5107(4)$	Cl2--Cu2--Cl1A	$112.619(15)$
Cl2--Cu1C	$2.2228(4)$	N2B--Cu2--Cu1	$89.94(4)$
N2--Cu2D	$2.0022(13)$	Cl1--Cu2--Cu1	$49.894(11)$
Cu1--Cl1--Cu2C	$121.732(18)$	Cl2--Cu2--Cu1	$154.113(13)$
Cu2--Cl1--Cu2C	$113.612(15)$	Cl1A--Cu2--Cu1	$73.751(11)$
Cu1C--Cl2--Cu2	$90.642(16)$	Cu1--Cl1--Cu2	$79.176(13)$

Symmetry codes: A) $x - 1/2, -y + 1/2, -z + 1$; B) $-x + 1, y + 1/2, -z + 1/2$; C) $x + 1/2, -y + 1/2, -z + 1$; D) $-x + 1, y - 1/2, -z + 1/2$.

Table 3. Selected bond lengths / Å and bond angles / ° for **2**.

Cu1–N1	1.918(4)	N1–Cu1–N2A	151.75(18)
Cu1–N2A	1.921(4)	N1–Cu1–O1	99.85(19)
Cu1–O1	2.372(7)	N2A–Cu1–O1	102.87(19)
N2–Cu1B	1.921(4)		

Symmetry codes: A) $-x + 1/2, y - 1/2, -z + 3/2$; B) $-x + 1/2, y + 1/2, -z + 3/2$.

2.3116(4) Å. Cu2 is coordinated by one N atom from the bpp ligand and three chloride ions, forming a tetrahedral geometry with the Cu2–N bond length of 2.0022(13) Å and the Cu2–Cl bond lengths in the range of 2.3465(4)–2.5107(4) Å. The Cu1...Cu2 separation is 2.9685(3) Å. As depicted in figure 1a, there are two

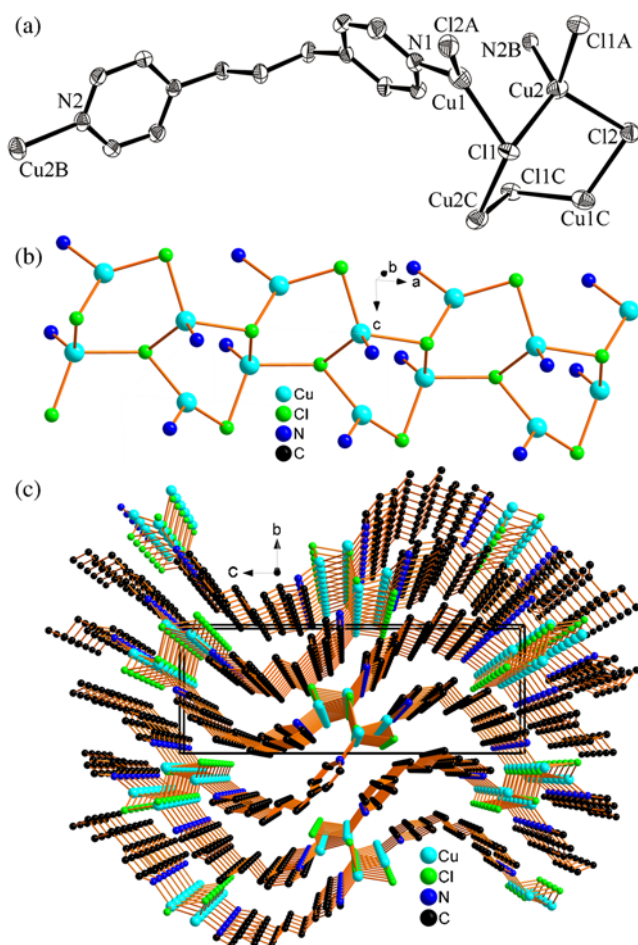


Figure 1. (a) Molecular structure of **1** with thermal ellipsoids drawn at the 50% probability level. Symmetry codes: A) $x - 1/2, -y + 1/2, -z + 1$; B) $-x + 1, y + 1/2, -z + 1/2$; C) $x + 1/2, -y + 1/2, -z + 1$. (b) A view of the inorganic [Cu₂Cl₂]_n ribbon in **1**. (c) A view of the three-dimensional structure of **1** viewed down the axis *a*. Hydrogen atoms are omitted for clarity.

different kinds of chloride ions. Cl1 acts as a μ_3 -bridge to link three Cu(I) ions. However, Cl2 behaves as a μ_2 -bridge connecting two Cu(I) ions. The two kinds of Cu(I) ions are consolidated by the two types of Cl[−] ions to build a one-dimensional inorganic [Cu₂Cl₂]_n ribbon (figure 1b). Each ribbon is further linked to another four ones by the bpp ligands to construct a three-dimensional MOF (figure 1c).

Topologically, Cu1 and Cu2 ions in the framework of **1** act as 3-connecting and 4-connecting nodes, respectively. The bpp ligands and Cl2 act as simple bridges between metal atoms, while Cl1 coordinates to three Cu(I) ions. This gives an overall 3,3,4-connected 3-nodal 3D network as shown in figure 2, which has the point symbol of (5.8²)(5².8³.9)(5².8).

The single-crystal X-ray diffraction analysis revealed that there are one Cu(I) center, one bpp ligand and half sulfate ion in the asymmetric unit of **2** as shown in figure 3a. Each Cu(I) ion is coordinated by two bpp ligands, and each bpp ligand in turn links two Cu(I) ions, resulting in the formation of a one-dimensional wave-like chain with the Cu–N bond lengths of 1.918(4) and 1.921(4) Å and the N–Cu–N angle of 151.75(19)°. The neighboring chains interact with each other side-by-side by SO₄^{2−} ions through weak Cu–O bonds (2.372(7) and 2.795(2) Å) which are comparable to those reported in documents.^{32–34} This leads to the formation of a porous two-dimensional sheet, which presents a flask-stacking appearance as shown in figure 3b and figure S7. The lattice DMF and H₂O molecules are filled in the voids.

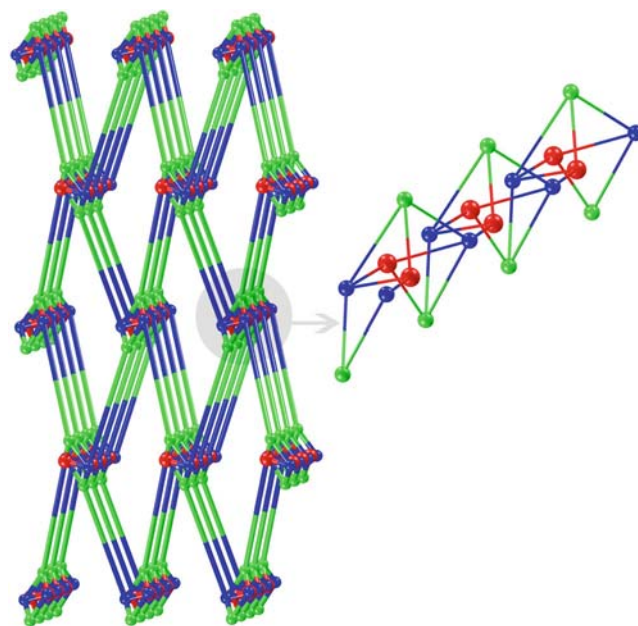


Figure 2. A topological view of **1**. Blue, green and red spheres represent Cu1, Cu2 and Cl1, respectively.

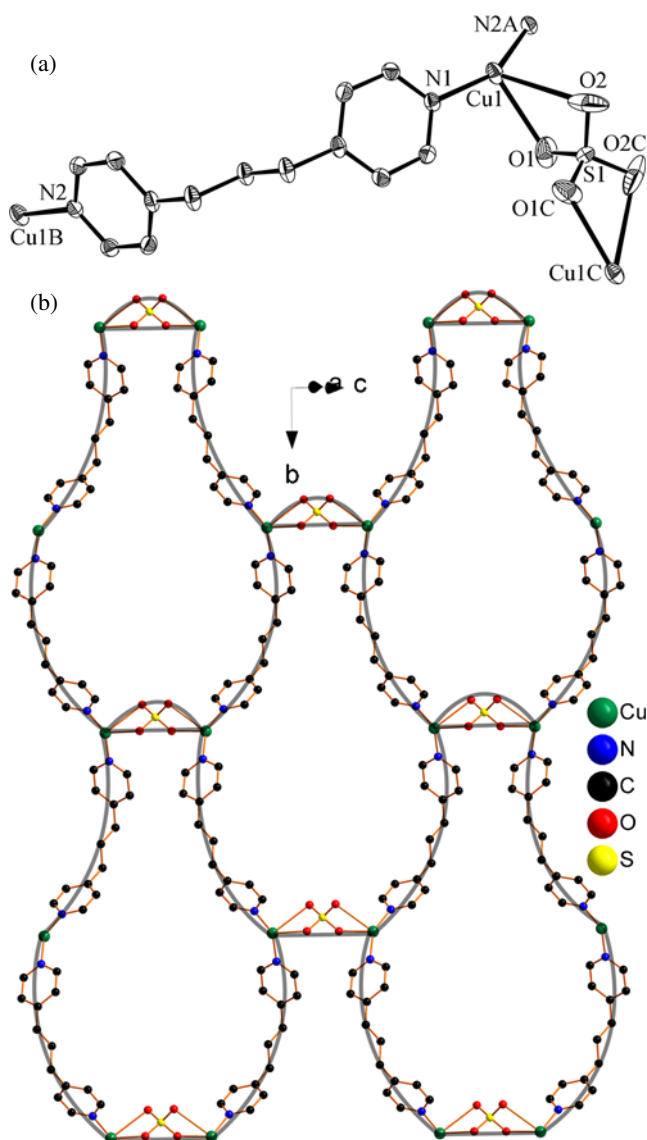


Figure 3. (a) Molecular structure of **2** with thermal ellipsoids drawn at the 30% probability level. Symmetry codes: A) $-x + 1/2, y - 1/2, -z + 3/2$; B) $-x + 1/2, y + 1/2, -z + 3/2$; C) $-x, y, -z + 1/2$. (b) Two-dimensional sheet of **2** with a schematic show of the flask-stacking appearance. All hydrogen atoms are omitted for clarity.

4. Conclusions

With the aim of tuning the structure of targeted metal-organic frameworks (MOFs) by the synergistic use of inorganic and organic linkers, we managed to separate two coordination frameworks of Cu(I) bearing the same organic linker of 3-bis(4-pyridyl)propane, but with different inorganic linkers. It revealed that the different inorganic linkers have an important role in the construction of this kind of coordination frameworks. The introduction of chloride anion as inorganic linker led to the formation of novel inorganic one-dimensional $[\text{Cu}_2\text{Cl}_2]$ ribbons, which are further linked

by the organic linker of bpp to form a three-dimensional metal-organic framework. The change of chloride into sulfate anions gave a two-dimensional framework with flask-stacking appearance, which is formed from the connection of one-dimensional $-\text{Cu}-\text{bpp}-\text{Cu}-$ chains by the inorganic sulfate linkers through weak coordination Cu–O bonds. It provides a strategy for preparing new kinds of coordination frameworks by the synergistic use of organic and inorganic linkers.

Supplementary Information (SI)

Crystallographic data for the two structures in this paper have been deposited in the Cambridge Crystallographic Database Center, CCDC, 12 Union Road, Cambridge CB21EZ, UK. Copies of the data can be obtained free of charge on quoting the depository number CCDC-1418270 for **1** and 1418165 for **2** (Fax: +44-1223-336-033; E-mail: deposit@ccdc.cam.ac.uk, <http://www.ccdc.cam.ac.uk>). IR spectra (figures S1, S2), TG (figures S3, S4), XRD (figures S5, S6) and the Space-filling diagram of the two-dimensional sheet of **2** (figure S7) are given in the supplementary information, which is available at www.ias.ac.in/chemsci.

Acknowledgement

The authors thank the financial support by National Natural Foundation of China (grant no. 21261004), Guangxi Natural Science Foundation of China (grant no. 2013GXNSFGA019008 and 2013GXNSFAA019039).

References

- Vishnoi P, Kalita A C and Murugavel R 2014 *J. Chem. Sci.* **126** 1385
- Tripathi S, Srirambalaji R, Singh N and Anantharaman G 2014 *J. Chem. Sci.* **126** 1423
- Janiak C 2003 *Dalton Trans.* **2** 781
- Rogez G, Viart N and Drillon M 2010 *Angew. Chem. Int. Ed.* **49** 1921
- Yu L, Wang Z, Wu J, Tu S and Ding K 2010 *Angew. Chem. Int. Ed.* **49** 3627
- Li J and Zhang C 2015 *J. Chem. Sci.* **127** 1871
- Suresh P and Prabusankar G 2014 *J. Chem. Sci.* **126** 1409
- Yoon M, Srirambalaji R and Kim K 2012 *Chem. Rev.* **112** 1196
- Sumida K, Rogow D L, Mason J A, McDonald T M, Bloch E D, Herm Z R, Bae T-H and Long J R 2012 *Chem. Rev.* **112** 724
- Zhou H-C, Long J R and Yaghi O M 2012 *Chem. Rev.* **112** 673
- Arauzo A, Lazarescu A, Shova S, Bartolome E, Cases R, Luzon J, Bartolome J and Turta C 2014 *Dalton Trans.* **43** 12342

12. Huck W T S 2005 *Chem. Commun.* 4143
13. Näther C and Jeß I 2004 *Eur. J. Inorg. Chem.* 2868
14. Serre C, Millange F, Thouvenot C, Noguès M, Marsolier G, Louër D and Férey G 2002 *J. Am. Chem. Soc.* **124** 13519
15. Wang Y J, Li H H, Chen Z R, Huang C C, Huang X H, Feng M and Lin Y 2008 *Cryst. Eng. Comm.* **10** 770
16. Mellot-Draznieks C, Serre C, Surblé S, Audebrand N and Férey G 2005 *J. Am. Chem. Soc.* **127** 16273
17. Wu Y, Kobayashi A, Halder G J, Peterson V K, Chapman K W, Lock N, Southon P D and Kepert C J 2008 *Angew. Chem. Int. Ed.* **47** 8929
18. Reger D L, Debreczeni A and Smith M D 2011 *Inorg. Chem.* **50** 11754
19. Kornienko N, Zhao Y, Kley C S, Zhu C, Kim D, Lin S, Chang C J, Yaghi O M and Yang P 2015 *J. Am. Chem. Soc.* **137** 14129
20. Wang L-F, Qiu J-Z, Liu J-L, Chen Y-C, Jia J-H, Jover J, Ruiz E and Tong M-L 2015 *Chem. Commun.* **51** 15358
21. Pfeiffermann M, Dong R, Graf R, Zajackowski W, Gorelik T, Pisula W, Narita A, Müllen K and Feng X 2015 *J. Am. Chem. Soc.* **137** 14525
22. Pal T K, Katoch R, Garg A and Bharadwaj P K 2015 *Cryst. Growth Des.* **15** 4526
23. Singh D and Baruah J B 2012 *Cryst. Growth Des.* **12** 2109
24. Pardo R, Zayat M and Levy D 2011 *Chem. Soc. Rev.* **40** 672
25. Sheldrick G M 1997 SHELXTL NT: Version version 5.1, University of Göttingen, Göttingen, Germany
26. Khanderi J, Contiu C, Engstler J, Hoffmann R C, Schneider J J, Drochner A and Vogel H 2011 *Nanoscale* **3** 1102
27. Zhu T, Hao J, Fu L, Li J and Liu Z 2005 *React. Kinet. Catal. Lett.* **84** 61
28. Pastoriza-Santos I and Liz-Marzán L M 1999 *Langmuir* **15** 948
29. Chiba M, Thanh M N, Hasegawa Y, Obora Y, Kawasaki H and Yonezawa T 2015 *J. Mat. Chem. C* **3** 514
30. Liu X, Li C, Xu J, Lv J, Zhu M, Guo Y, Cui S, Liu H, Wang S and Li Y 2008 *J. Phys. Chem. C* **112** 10778
31. Li D, Jones E M, Sawaya M R, Furukawa H, Luo F, Ivanova M, Sievers S A, Wang W, Yaghi O M, Liu C and Eisenberg D S 2014 *J. Am. Chem. Soc.* **136** 18044
32. Min K S, Park A H, Shin J W, Rowthu S R, Kim S K and Ryoo J J 2010 *Dalton Trans.* **39** 8741
33. Khandar A A, Cardin C, Hosseini-Yazdi S A, McGrady J, Abedi M, Zarei S A and Gan Y 2010 *Inorg. Chim. Acta* **363** 4080
34. Akhuli B and Ghosh P 2013 *Dalton Trans.* **42** 5818